THE RIM OF THE SOUTH POLE-AITKEN BASIN: NEW EMPIRICAL EVIDENCE

Charles J. Byrne, Image Again, 39 Brandywine Way, Middletown, NJ 07748, charles.byrne@verizon.net.

Introduction: Early interpretations of the Lunar Orbiter images of the South Pole-Aitken Basin (SPA) identified separate mountain ranges before they were perceived as a continuous rim of a deep crater. This interpretation was confirmed when topographic information was obtained from the laser altimeter of the Clementine spacecraft, although it could not measure the part of the feature near the South Pole, below 78° S. As better topographic data was obtained from Kaguya and the Lunar Reconnaissance Orbiter, the elliptical nature of the crater and the boundary range became clear [1]. The SPA was seen to be caused by an oblique impact, with the impactor approaching at an angle of at least 45° from the vertical (not more than 45° from the horizontal).

New evidence: Two convergent sources of evidence are presented here:

- A 3-D simulation of an oblique impact of a projectile with approximately the right kinetic energy to produce such a large basin (Figure 1)
- A new analysis examines the relation between the topography of the SPA and the far side bulge (Figure 2).

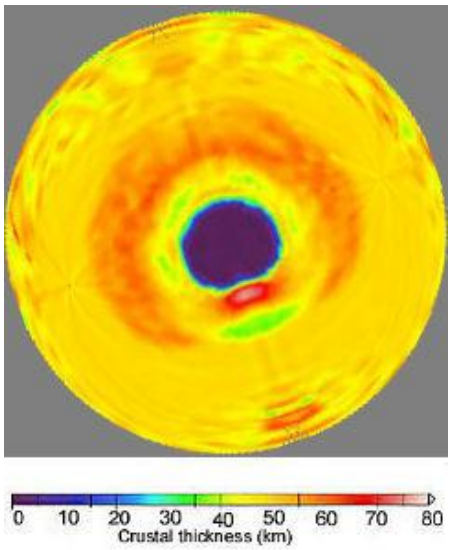

Figure 1: This topographic map is a 3-D simulation of the SPA [2, Figure 7B of the Supplementary Online Material]. The impact is of a projectile 250 km in diameter entering from the southeast [2]. The simulated data is reprojected to Lambert equal area, range 120°, North to the top [3, Appendix C]. Other parameters are described in the text.

3-D Simulation: A series of 3-D simulations of parametric variations of the impact that formed the SPA surface topology were done to support an analysis of the SPA magnetic anomaly by Wieczorek, Weiss, and Stewart [2]. The simulation case chosen to be most similar to the empirical data of Figure 2 (Figure 7B of [2] is shown in Figure 1. The approach angle of the impactor was 45 ° from the vertical, from the southeast, 18.8° counterclockwise from the south and the center coordinates of the cavity were set at 52° S, 171° W to match the center and arc of the magnetic anomaly [2] (which was downstream of the center). Figure 1 shows the initial state of the SPA, before compensation.

Empirical map of the SPA: Until recently, there has been no empirical verification of the rim and ejecta field of the SPA. In [3], a topographic map of the rim and ejecta field of the SPA was produced by subtracting models of the Near Side Megabasin (NSM) and the Chaplygin-Mandel'shtam Basin (CM) [4] from the current topography (see Figure 2). This figure shows that the rim of the SPA is much larger than its peak ring, which has been thought to be the main ring.

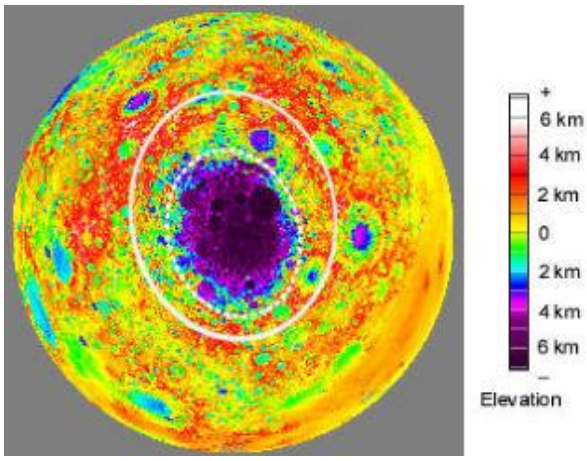

Figure 2: This topographic map has the same projection and other parameters as Figure 1. It is based on Kaguya topography [3] but models of the Near Side Megabasin [4] and the Chaplygin-Mandelshtam Basin [4] have been removed from that topography. The **white dotted ellipse** is the edge of the Apparent Crater, beyond the modest rise of the peak ring, formerly thought to be the main ring. The **white solid ellipse** is the rim crest (see text). Base map: JAXA, Kaguya [5], reprojected in [3, Appendix C].

Figure 2 shows the Moon as if the two subtracted basins had not happened. The major remaining patterns

are due to the SPA crater, its rim, and its ejecta field. All subsequent impacts are also shown. Although the rim crest is shown as an ellipse in Figure 2, it actually is more complex. The following sections show the maps of the current topography and the model of earlier features that were used to produce Figure 2.

Current topography of the SPA area: To reveal the part of the Moon's topography due to the SPA, one starts with the current Moon's topography (Figure 3).

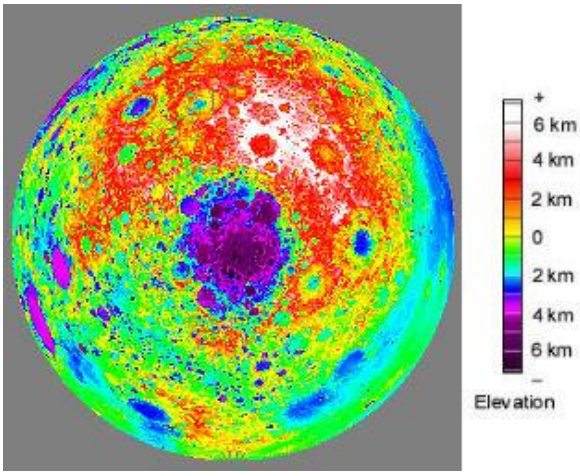

Figure 3: The Moon's current topography from 1° elevation data produced by the laser altimeter (LALT) data of the Kaguya mission [5]. This map is a Lambert equal area projection, 120° range, centered at 52° S, 171° E (the center of the SPA's cavity). The highest elevations (white) are around the Korolev Basin and neighboring features. The lower third of the map shows part of the southern near side up to 12° S. Data source: JAXA, Kaguya, LALT [5]. Projection and false color scale by the current author [3, Appendix C].

The model of earlier features: Although large, the crater of the SPA is not large enough to produce the entire far side bulge, nor is the far side bulge symmetric with the SPA cavity. Although there are various hypotheses of how the far side bulge was formed, this model of the NSM is the best quantitative model of the far side bulge and the large scale topography of the near side as well. The basic parameters of the model are the center coordinates, the apparent diameter and the apparent diameter and depth of a peak ring, if there is one. Although the model is limited to nearly circular features, a small degree of ellipticity can be accommodated. The NSM antipode is in the Korolev basin. The map of Figure 4 has the same projection parameters as in Figures 1, 2 and 3.

Removal of the basins underlying the SPA: The empirical map of the SPA (Figure 2) is derived by simple subtraction of the topography of Figure 4 from that of Figure 3. The models of the NSM and CM were derived independently of the simulation map.

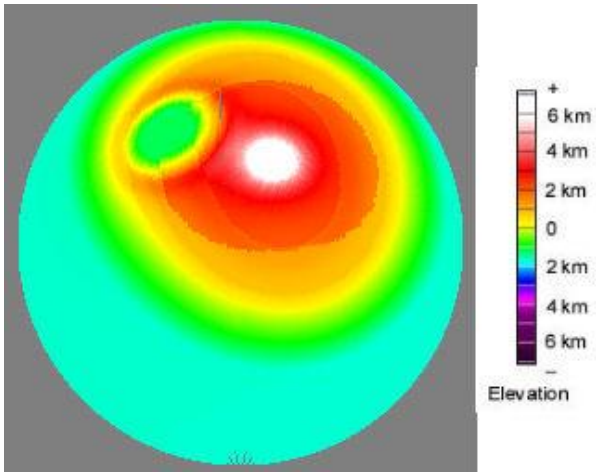

Figure 4: This map shows models of the Near Side Magabasin and a smaller impact feature, the Chaplygin-Mandle'shtam basin which is believed to be later than the NSM but earlier than the SPA. The white area encloses the antipode of the NSM at 8° S and 156° W. Descriptions and parameters of the NSM and CM are from [3, Appendix C], 4].

Conclusion: The 3-D simulation in Figure 1 and the revealed empirical evidence in Figure 2 are in excellent qualitative agreement (and nearly quantitative agreement). The mountain arcs thought to be the rim are actually the peak ring, the downstream rim arcs being further out. Upstream, the rim arc is closer to the peak ring. New definitions of terms like rim, main ring, and peak ring will be needed for oblique impacts.

The lack of any pattern in Figure 2 similar to the NSM or CM, after their subtraction, confirms the assumed linearity of the superposition, the realism of the resulting SPA topography, and the realism of the NSM itself as well as the extension of the scaled model, derived from large basins, to such a giant impact feature.

References:

[1] Garrick-Bethell, I., Zuber, M.T. (2009) Elliptical structure of the lunar South Pole-Aitken Basin, Icarus 204, 399–408.

[2] Wieczorek, M. A., Weiss, B. P., and Stewart, S. T. (2012) An impactor origin for lunar magnetic anomalies, Science, Vol.335, 2012 and Supplementary Online Material.

[3] Byrne, C. J. (2015) The Moon's Largest Craters and Basins: images and topographic maps from LRO, GRAIL, and Kaguya, Springer, 2015.

[4] Byrne, C. J. (2013) The Moon's Near Side Megabasin and Far Side Bulge, Springer, 2013.

[5] Japan Aerospace Exploration Agency (JAXA), Result of Kaguya, (1) The global 1 degree grid topographic data, website: http://www.selene.jaxa.jp/en/science/LALT/The_lunar_topographic_data_e.htm.